

# Discovery of a Highly Potent, Orally Active Mitosis/Angiogenesis Inhibitor R1530 for the Treatment of Solid Tumors

Jin-Jun Liu,\*,† Brian Higgins,‡ Grace Ju,‡ Kenneth Kolinsky,‡ Kin-Chun Luk,\*,† Kathryn Packman,‡ Giacomo Pizzolato,† Yi Ren,§ Kshitij Thakkar,† Christian Tovar,‡ Zhuming Zhang,† and Peter M. Wovkulich\*,†

<sup>†</sup>Discovery Chemistry, <sup>‡</sup>Discovery Oncology, and <sup>§</sup>Chemical Synthesis, Hoffmann-La Roche Inc., 340 Kingsland Street, Nutley, New Jersey 07110, United States

Supporting Information

ABSTRACT: A new series of 7,8-disubstituted pyrazolobenzodiazepines based on the lead compound 1 have been synthesized and evaluated for their effects on mitosis and angiogenesis. Described herein is the design, synthesis, SAR, and antitumor activity of these compounds leading to the identification of R1530, which was selected for clinical evaluation.

**KEYWORDS:** pyrazolobenzodiazepines, mitosis/angiogenesis inhibitor, antitumor effect, VGFr-2, FGFr and PDGFr-β

ngiogenesis, the growth of new blood vessels, is an Anglogenesis, the grown of his tumors. Therapeutic regimens in oncology frequently employ combinations of agents in an attempt to maximize efficacy. Targeting angiogenesis pathways 1-9 and mitotic processes are among the many combinations currently undergoing clinical study and, from recent reports, appear to offer some promise of improved clinical response. We were interested in further exploring our new pyrazolobenzodiazepine kinase inhibitor template in this context.

We have recently described the discovery of pyrazolobenzodiazepines<sup>14</sup> as ATP competitive kinase inhibitors and their optimization to compound 1.15 Compound 1 showed potent inhibitory activities against kinases, such as cyclin-dependent kinases (CDKs) 2 and 4, and angiogenesis-related growth factor receptor tyrosine kinases, such as kinase insert domain receptor (KDR), fibroblast growth factor receptor (FGFr), platelet-derived growth factor receptor (PDGFr), and epidermal growth factor receptor (EGFr). It also exhibited potent in vitro antiproliferative activity in a wide range of human tumor cell lines derived from different tissue types. While the antiangiogenic activities appear to be separate from the antiproliferative activities, the precise target for the antiproliferative activity remains elusive. The noteworthy antiangiogenic activity and antitumor activity of compound 1 in mouse models<sup>9,16</sup> proved a compelling argument for further investigation. However, an unattractive ADMET profile rendered the compound less interesting for human evaluation. We then directed our attention to modifications at the 7- and 8positions on the fused benzene ring in an attempt to improve on the kinase inhibitory activities and ADME properties and eventually identified compound 2 (R1530) as a highly potent, orally bioavailable, dual-acting mitosis/angiogenesis inhibitor for the treatment of solid tumors. These biological attributes of R1530 have been explicitly discussed in prior reports. 25,26 We describe herein the synthesis and biological evaluation of R1530.

Our early preparations of R1530 were part of an effort designed to probe the structure-activity relationship of disubstitution at the 7- and 8-position (Figure 1). For maximal

$$H_2N$$
 $H_2N$ 
 $H_2N$ 
 $H_2N$ 
 $H_3N$ 
 $H_2N$ 
 $H_3N$ 
 $H_3N$ 

Figure 1.

adaptability with respect to scalability and convergence in the early stages, we developed two general routes. Commercially available disubstituted anilines 3 were reacted with 2chlorobenzonitrile 4 via the Sugasawa reaction 17,18 in the presence of BCl<sub>3</sub> and GaCl<sub>3</sub> in toluene to give the intermediate imines 5, which formed the corresponding benzodiazepines 6 by treatment with MeOCOCH<sub>2</sub>NH<sub>3</sub>Cl in a mixture of AcOH and iPrOH. 7-Alkoxy-8-fluoro imines 5 derivatives were obtained by treatment of the corresponding difluoro imines  $\mathbf{5}$  (R<sup>1</sup>, R<sup>2</sup> = F) with the appropriate alcohols (R<sup>2</sup>

Received: November 8, 2012 Accepted: January 15, 2013 Published: January 15, 2013

= OR) and NaOR. Benzodiazepines **6** were then converted to the desired 7,8-disubstituted pyrazolobenzodiazepine **2** in three steps as described previously (Scheme 1).<sup>15</sup> Alternatively,

#### Scheme 1. Synthesis of Compound 2<sup>a</sup>

$$R^{2} \longrightarrow NH_{2}$$

$$R^{1} \longrightarrow NH_{2}$$

$$R^{1} \longrightarrow NH_{2}$$

$$R^{1} \longrightarrow NH_{2}$$

$$Sa: R^{1}, R^{2} = F$$

$$Sb: R^{1} = F, R^{2} = OF$$

$$CI \longrightarrow N$$

$$CI \longrightarrow N$$

$$CI \longrightarrow N$$

$$R^{2} \longrightarrow NH_{2}$$

$$Sb: R^{1} = F, R^{2} = OF$$

$$R^{2} \longrightarrow NH_{2}$$

$$Sb: R^{1} = F, R^{2} = OF$$

$$R^{2} \longrightarrow NH_{2}$$

$$Sb: R^{1} = F, R^{2} = OF$$

$$R^{2} \longrightarrow NH_{2}$$

$$Sb: R^{1} = F, R^{2} = OF$$

$$R^{2} \longrightarrow NH_{2}$$

$$Sb: R^{1} = F, R^{2} = OF$$

$$R^{2} \longrightarrow NH_{2}$$

$$Sb: R^{1} = F, R^{2} = OF$$

$$R^{2} \longrightarrow NH_{2}$$

$$Sb: R^{1} = F, R^{2} = OF$$

$$R^{2} \longrightarrow NH_{2}$$

$$Sb: R^{1} = F, R^{2} = OF$$

$$R^{2} \longrightarrow NH_{2}$$

$$Sb: R^{1} = F, R^{2} = OF$$

$$R^{2} \longrightarrow NH_{2}$$

$$Sb: R^{1} = F, R^{2} = OF$$

$$R^{2} \longrightarrow NH_{2}$$

$$Sb: R^{1} = F, R^{2} = OF$$

$$R^{2} \longrightarrow NH_{2}$$

$$Sb: R^{1} = F, R^{2} = OF$$

$$R^{2} \longrightarrow NH_{2}$$

$$Sb: R^{1} = F, R^{2} = OF$$

$$R^{2} \longrightarrow NH_{2}$$

$$Sb: R^{1} = F, R^{2} = OF$$

$$R^{2} \longrightarrow NH_{2}$$

$$Sb: R^{1} = F, R^{2} = OF$$

$$R^{2} \longrightarrow NH_{2}$$

$$Sb: R^{1} = F, R^{2} = OF$$

$$R^{2} \longrightarrow NH_{2}$$

$$Sb: R^{1} = F, R^{2} = OF$$

$$R^{2} \longrightarrow NH_{2}$$

$$Sb: R^{2} \longrightarrow NH_{2}$$

$$Sb:$$

"Reagents and conditions: (a) BCl<sub>3</sub>/GaCl<sub>3</sub>/toluene, reflux. (b) NaOR/ROH, reflux. (c) MeOCOCH<sub>2</sub>NH<sub>3</sub>Cl/AcOH/iPrOH, reflux. (d) MeCHO. (e) Hydrazine. (f) Air oxidation, DMSO, 150 °C.

compounds 2 could be prepared in a more convergent manner as outlined in Scheme 2. A microwave-promoted coupling

## Scheme 2. Convergent Synthesis of Compound 2<sup>a</sup>

"Reagents and conditions: (a) BCl<sub>3</sub>/GaCl<sub>3</sub>/toluene, reflux. (b) MnO<sub>2</sub>· (c) MeOH/NAOMe, reflux. (d) TEA, 80 °C, 3 h. (e) CuCl<sub>2</sub>/NaNO<sub>2</sub>/HCl (49%, two steps). (f) NaOH. (g) ClCOOEt/TEA/NaN<sub>3</sub>. (h) HCl, 110 °C, 2 h (50%, three steps). (i) TsOH/iPrOH/microwave, 170 °C, 15 min. (j) DIBAH/THF/(dppp)NiCl<sub>2</sub>.

reaction between disubstituted benzophenone 9 and 1-allyl-5-chloro-3-methyl-1H-pyrazol-4-ylamine 13 followed by removal of the allyl group using the general method described in the literature provided 2 in moderate yields. The disubstituted benzophenones 8 were made from commercially available disubstituted anilines 3 by reacting with 2-chlorobenzaldehyde 7 using BCl<sub>3</sub> and GaCl<sub>3</sub> as catalysts, followed by oxidation with MnO<sub>2</sub>. The 8-alkoxy benzophenones 9 were conveniently derived from the difluoro-substituted benzophenone 8 ( $R^1 = R^2 = F$ ) by the regioselective replacement reaction with alcohols in the presence of base. The 1-allyl-5-chloro-3-methyl-1H-pyrazol-4-ylamine 13 was prepared by condensation of 2-cyano-3-ethoxy-but-2-enoic acid ethyl ester 10 and allyl-hydrazine 11 followed by diazotization, chloride formation, and subsequent Curtius reaction. The convergent route represents a quick

way to access a variety of substituent groups on the benzene ring, while the linear synthesis gives a better overall yield for a specific analogue.<sup>22</sup>

By using these methods, a broad range of 7,8-disubstituted pyrazolobenzodiazepine analogues were evaluated (data not shown), of which R1530 (compound 2) emerged based on its biological activities and pharmacokinetics (PK) properties

Of particular interest, R1530 as compared to the monosubstituted compound 1 showed stronger inhibitory activities against angiogenesis-related receptor tyrosine kinases (KDR, FGFr) and weaker activities against CDK2 and -4 (Table 1), indicating the feasibility of improving potency and selectivity for the angiogenesis-related kinases.

Table 1. Kinase Inhibition of Selected Mono- and 7,8-Disubstituted Pyrazolobenzodiazepines  $(IC_{50} \mu M)^a$ 

compd	KDR	FGFr1	CDK2	CDK4		
1	0.034	0.050	0.088	0.303		
2	0.010	0.028	1.330	>10		
<sup>a</sup> Values are the means of duplicate experiments. <sup>16</sup>						

R1530 was profiled first in an in-house panel of 30 kinases. In addition to confirming the previously mentioned kinases, this first round of profiling identified two kinases associated with G2/M phase activities, Aurora A (58 nM) and checkpoint kinase 2 (Chk2) (24 nM). The compound was then evaluated in an Ambit panel of 178 kinases, with  $K_{\rm d}$  values determined for those kinases showing >85% signal at 1  $\mu$ M<sup>23,24</sup> (Supplementary Table 1 in the Supporting Information).

The in vitro antiproliferative effects of R1530 were further evaluated by the tetrazolium dye assay (MTT) in human tumor cell lines originating from various human tumor tissues including breast, colon, lung, prostate, melanoma, and oral epidermoid (Supplementary Table 2 in the Supporting Information). R1530 exhibited potent in vitro antiproliferative activity in all of the tumor cell lines tested (IC<sub>50</sub> = 0.2-3.4μM). Because of its ability to inhibit the kinase activities of vascular endothelial growth factor receptor 2 (VGFr2), FGFr1, and PDGFr-\(\beta\), R1530 was further characterized for its effects on VEGF and bFGF-induced proliferation of human umbilical vein endothelial cells (HUVEC) and PDGF driven fibroblast proliferation. R1530 showed strong inhibition of VEGF and bFGF induced HUVEC proliferation ( $IC_{50} = 49$  and 118 nM); however, activity in the PDGF driven assay was less potent  $(IC_{50} = 688 \text{ nM}).$ 

R1530 disrupts cells in mitosis, an effect less consistent with the inhibition of CDK2 and CDK4 and more in line with the interference of tubulin polymerization and inhibition of checkpoint kinases. The working hypothesis of R1530 antitumor effect is unique and is classified as being the product of mitotic slippage, subsequently followed by induction of endoreduplication and the generation of polyploidy. The resultant effect of R1530 on cells is apoptosis (mitotic catastrophe) or senescence (Figure 2). These direct antitumor cell effects in combination with the antiangiogenic activity ultimately translate into potent in vivo efficacy. Normal proliferating cells were resistant to R1530 induced polyploidy. The control of the control

R1530 showed acceptable PK properties in multispecies. The single-dose PK of R1530 were generally similar among the mouse, rat, and monkey: following intravenous injection, the volume of distribution at steady state (Vdss) was generally high (1.59–3.22 L/kg), the total plasma clearance (CL) was

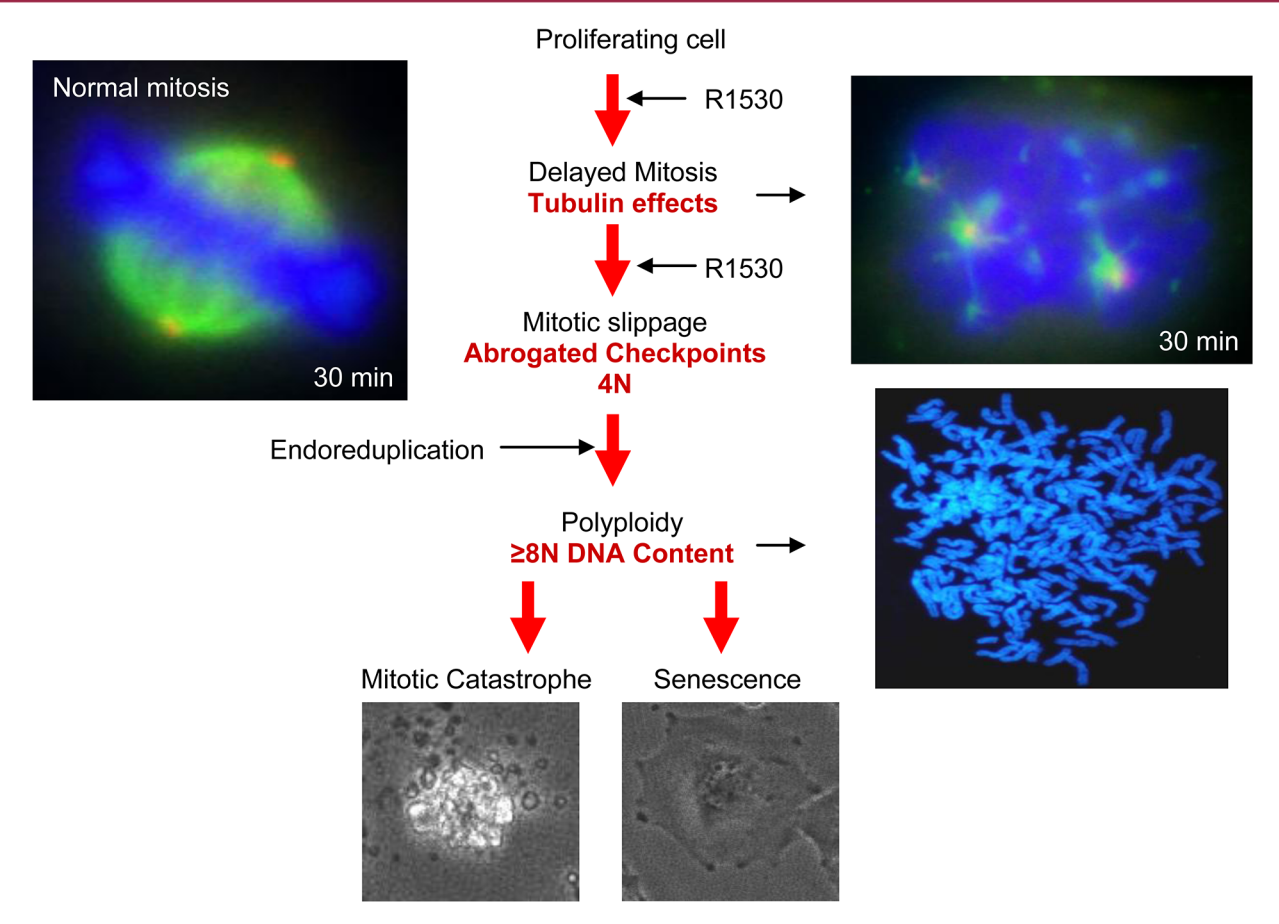


Figure 2. Working hypothesis of R1530 antitumor effect.

moderate to high (469–528 mL/kg/h), while the terminal elimination half-life ( $T_{1/2}$ ) was between 3 and 5 h (Table 2). Following single-dose oral administration, R1530 was generally well absorbed, with high oral bioavailability in rodents and moderate bioavailability in monkeys (Table 3).

Table 2. Single iv Dose PK of R1530

species	mouse	rat	monkey
dose (mg/kg)	5	5	1
CL (mL/kg/h)	528	527	469
Vss (L/kg)	3.12	3.22	1.59
half-life (h)	4.32	4.70	3.83

Table 3. Single Oral Dose PK of R1530

species	mouse	rat	monkey
dose (mg/kg)	25	50	10
$T_{\rm max}$ (h)	2	4-8	4-8
$C_{\text{max}} (\text{ng/mL})$	5070	5360	406
$AUC_{0-24h}\;(ng\;h/mL)$	46700	86300	4820
F (%)	96.9	88.7	22.1

Efficacy studies of R1530 were conducted in mice utilizing various human tumor xenograft models. Animals were dosed orally, once a day (qd) at 1.56, 25, or 50 mg/kg. R1530 produced significant tumor growth inhibition in all models tested, with regression observed in all models tested at a 50 mg/kg dose. In the three models where 1/2 MTD (25 mg/kg) of R1530 was tested, regressions were observed in two out of three models (MDA-MB-435, Figure 3; LoVo, Supplementary

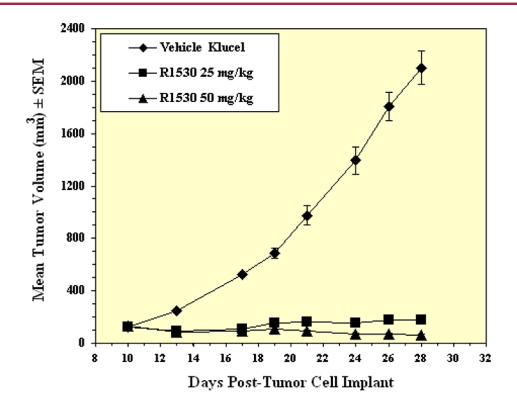


Figure 3. Efficacy studies of R1530 in mice utilizing MDA-MB-435 human tumor xenograft model.

Figure 1 in the Supporting Information) with the third (22rv1, Supplementary Figure 2 in the Supporting Information) yielding 98% tumor growth inhibition (TGI). The 1.56 mg/kg dose was not efficacious in either the HCT116 (Supplementary Figure 3 in the Supporting Information) or the A549 model (Supplementary Figure 4 in the Supporting Information). No signs of toxicity were noted in any of the dose groups as assessed by measuring changes in body weight and gross observation of individual animals (data not shown). There was a biologically significant increase in survival ( $\geq$ 25%) in all groups dosed with 25 or 50 mg/kg of R1530 regardless of the xenograft models tested.

The in vivo studies demonstrated that R1530 has notable antitumor activity across a broad range of human xenograft

models, with minimal toxicity, and provided compelling support for further evaluation of R1530 in humans. R1530 disrupts normal tubulin dynamics inducing a delay in the transition of mitosis. Because of R1530 inhibitory effects on the checkpoint machinery, cells slip through the mitotic block without the proper partitioning of DNA and cytokinesis. Endoreduplication occurs, and the cells ultimately undergo cell death via mitotic catastrophe or cellular senescence.

To provide the larger quantities of material needed for the toxicology and clinical formulation studies, a comparison was made of the two methods described above for the preparation of R1530. In the convergent method, the synthesis began with commercially available 3,4-difluoro-aniline 14, which on reaction with 2-chlorobenzaldehyde 7 and subsequent oxidation gave benzophenone 15 in 86% yield (Scheme 3).

Scheme 3. Large Scale Synthesis of R1530<sup>a</sup>

"Reagents and conditions: (a) PhBCl<sub>2</sub>/TEA/NaOH aq. (b) MnO<sub>2</sub> (86%, two steps). (c) MeOH/NaOMe, reflux, 80 min, 97%. (d) TsOH/iPrOH/microwave, 170 °C, 15 min, 45%. (e) DIBAH/THF/ (dppp)NiCl<sub>2</sub>, 29%. (f) BCl<sub>3</sub>/GaCl<sub>3</sub>/toluene, reflux. (g) Na-OMe/ MeOH/t-amyl alcohol, reflux (52%, two steps). (h) MeO-COCH<sub>2</sub>NH<sub>3</sub>Cl/AcOH/iPrOH, reflux, 91%. (i) POCl<sub>3</sub> (1.5 equiv)/DIPEA (6.0 equiv)/Triazole (6.0 equiv)/THF, 10 °C to rt. (j) MeOH/NaOMe (7.0 equiv)/MeOH, reflux, 18 h (98%, two steps). (k) DMA(OMe)<sub>2</sub> (2.0 eq, slow addition), DMF, 130 °C, 20 h. (l) N<sub>2</sub>H<sub>4</sub> (6.0 equiv)/L-ascorbic acid (0.02 equiv)/CH<sub>2</sub>Cl<sub>2</sub>/MeOH, rt, 20 h, or toluene, reflux (72%, two steps). 30–35% overall yield from compound 14.

Introduction of the 8-methoxy group was accomplished by the regioselective fluoride displacement of benzophenone **15** using sodium methoxide in refluxing methanol to give ketone **9** in 97% yield. Microwave-promoted coupling of **9** plus 1-allyl-5-chloro-3-methyl-1*H*-pyrazol-4-ylamine **13** followed by deprotection gave R1530 in low yield for the two steps.

Alternatively, the linear route began with the Sugasawa reaction of 14 and 2-chloro-benzonitrile 4 followed by treatment with NaOMe in methanol gave imine 5b in 52% yield for the two steps. Treatment of imine 5b with glycine methyl ester hydrochloride in refluxing isopropanol-acetic acid produced the corresponding 7-fluoro-8-methoxy-benzodiazepine 16 in 91% yield. Benzodiazepine 16 was treated with 1,2,4-

triazole, diisopropylethylamine, and phosphorus oxychloride, followed by sodium methoxide in methanol to give iminomethyl ether 17. Slow addition of N<sub>1</sub>N-dimethylacetamide dimethyl acetal (DMA-DMA, 2 equiv) to a solution of 17 in DMF at 130 °C, followed by an additional 24 h of heating at 130 °C, resulted in the formation of the acylated intermediate. The DMF was removed under reduced pressure, and the residue was treated with hydrazine in a mixture of dichloromethane and methanol at room temperature or in toluene at 110 °C. The crude R1530 was obtained by precipitation, triturated with hot 1,2-difluorobenzene, then dissolved in acetone, and filtered to remove solids. After solvent exchange to isopropyl acetate, the addition of heptane followed by filtration gave the title compound, R1530, in 72% yield from 16. This linear process has been successfully utilized by our Chemical Synthesis Department to produce 3.4 kg of clinical material with 30-35% overall yield.

In summary, further exploration of the pyrazolobenzodiazepine template at the 7- and 8-positions has led to the discovery of R1530. Additional profiling of R1530 demonstrated the potent antiproliferative and proapoptotic activities as well as robust in vivo efficacy. Two efficient synthetic processes were developed to make R1530 and its derivatives, and a seven-step synthesis was used for process chemistry with 30–35% overall yield. R1530 was selected for further evaluation in phase I clinical evaluations.

## ASSOCIATED CONTENT

# **S** Supporting Information

Experimental details for the synthesis and characterization of R1530. This material is available free of charge via the Internet at http://pubs.acs.org.

# AUTHOR INFORMATION

#### **Corresponding Author**

\*E-mail: jinzi06@gmail.com (J.-J.L.), kin-chun.luk@roche.com (K.-C.L.), or wovkuln24@verizon.net (P.M.W.).

#### Notes

The authors declare no competing financial interest.

### ■ ACKNOWLEDGMENTS

We thank Gino Sasso for <sup>1</sup>H NMR spectral analysis and NOE studies and Vance Bell, Richard Szypula, Theresa Burchfield, and Michael Lanyi for mass and IR spectral analysis. We thank members of the Discovery Oncology In Vivo Section for assistance with tumor efficacy studies, and Hong Yang and Daisy Carvajal for cell-based assay work.

# ABBREVIATIONS

KDR, kinase insert domain receptor, an alternative name for VGFr2; VGFr2, vascular endothelial growth factor receptor 2; FGFr, fibroblast growth factor receptors; PDGFr, platelet-derived growth factor receptors; EGFr, epidermal growth factor receptor; Chk2, checkpoint kinase 2; CDK, cyclin-dependent kinases; TGI, tumor growth inhibition; PK, pharmacokinetics; CL, clearance; Vss, volume of distribution;  $T_{\rm max}$ , time of maximum concentration;  $C_{\rm max}$ , maximum concentration; AUC, area under curve; F, measure of oral bioavilibility

## REFERENCES

(1) Folkman, J. The role of angiogenesis in tumor growth. Semin. Cancer Biol. 1992, 3, 65–71.

- (2) Folkman, J. Cancer Medicine; Williams and Wilkins: Baltimore, MD, 1997; pp 181-204.
- (3) Folkman, J. Anti-angiogenesis: New concept for therapy of solid tumors. *Ann. Surg.* **1972**, *175*, 409–416.
- (4) Folkman, J. Angiogenesis: An organizing principle for drug discovery? *Nat. Rev. Drug Discovery* **2007**, *6*, 273–286.
- (5) Ruegg, C.; Mutter, N. Anti-angiogenic therapies in cancer: achievements and open questions. *Bull. Cancer* **2007**, *94*, 753–762.
- (6) Carmeliet, P.; Jain, R. K. Angiogenesis in cancer and other diseases. *Nature* **2000**, *407*, 249.
- (7) Tonini, T.; Rossi, F.; Claudio, P. P. Molecular basis of angiogenesis and cancer. *Oncogene* **2003**, 22, 6549.
- (8) Risau, W. Mechanisms of angiogenesis. Nature 1997, 386, 671.
- (9) Muruganandham, M.; Lupu, M.; Dyke, J. P.; Matei, C.; Linn, M.; Packman, K.; Kolinsky, K.; Higgins, B.; Koutcher, J. A. Preclinical evaluation of tumor microvascular response to a novel antiangiogenic/antitumor agent RO0281501 by dynamic contrast-enhanced MRI at 1.5 T. *Mol. Cancer Ther.* **2006**, *5*, 1950.
- (10) Sosman, J.; Puzanov, I. Combination targeted therapy in advanced renal cell carcinoma. *Cancer* **2009**, *115* (10, Suppl.), 2368–2375.
- (11) Pennell, N. A.; Lynch, T. J. Combined Inhibition of the VEGFR and EGFR Signaling Pathways in the Treatment of NSCLC. *Oncologist* **2009**, *14* (4), 399–411.
- (12) Ma, J.; Waxman, D. J. Combination of antiangiogenesis with chemotherapy for more effective cancer treatment. *Mol. Cancer Ther.* **2008**, *7* (12), 3670–3684.
- (13) Flaherty, K. T. The future of tyrosine kinase inhibitors: Single agent or combination? *Curr. Oncol. Rep.* **2008**, *10* (3), 264–270.
- (14) Sternbach, L. H. The benzodiazepine story. *Prog. Drug Res.* 1978, 22, 229–266.
- (15) Liu, J. J.; Daniewiski, I.; Ding, Q.; Higgins, B.; Ju, G.; Kolinsky, K.; Konzelmann, F.; Lukacs, C.; Pizzolato, G.; Rossman, P.; Swain, A.; Thakkar, K.; Wei, C.; Miklowski, D.; Yang, H.; Yin, X.; Wovkulich, P. M. Pyrazolobenzodiazepines: Part I. Synthesis and SAR of a potent class of kinase inhibitors. *Bioorg. Med. Chem. Lett.* **2010**, *20*, 5984–5987.
- (16) Higgins, B.; Kolinsky, K.; Yang, H.; Tovar, C.; Carvaial, D.; Yin, X.; Bachynsky, M.; Margolis, R.; Nevins, T.; Geng, W.; Lamb, M.; Linn, M.; Liu, J. J.; Wovkulich, P.; Packman, K.; Ju, G. In Vivo Activity of the Novel Dual Acting Mitotic and Angiogenesis Inhibitor RO0281501 (MAI) in the Rat Corneal Pocket and Rat Syngeneic Tumor Models. 17th AACR-NCI-EORTC Int. Conf. Mol. Targets Cancer Ther. 2005, Abstract B217.
- (17) Sasakura, K.; Torti, Y.; Sugasawa, T. Aminohaloborane in Organic Synthesis. X. A Convenient, Economical Exclusive ortho Substitution Reaction of N-Alkyl and N-Aminoalkyl Anilines. *Chem. Pharm. Bull.* **1985**, *33*, 1836–1842 and references therein.
- (18) Sugasawa, T.; Toyoda, T.; Adachi, M.; Sesakura, K. Aminohaloborane in organic synthesis. 1. Specific ortho substitution reaction of anilines. *J. Am. Chem. Soc.* **1978**, *100*, 4842.
- (19) Douglas, A. W.; Abramson, N. L.; Houpis, I. N.; Karady, S.; Molina, A.; Xavier, L. C.; Yasuda, N. *In situ* NMR spectroscopic studies of aniline ortho acylation ("sugasawa reaction"): The nature of reaction intermediates and Lewis acid influence on yield. *Tetrahedron Lett.* **1994**, *35* (37), 6807–6810.
- (20) Taniguchi, T.; Ogasawara, K. Facile and specific nickel-catalyzed de-N-allylation. *Tetrahedron Lett.* **1998**, *39*, 4679–4682.
- (21) Curtius, T. Uber Stickstoffwasserstoffsäure (Azoimid) N3H. Chem. Ber. 1890, 23, 3023.
- (22) Liu, J. J.; Luk, K.-C.; Pizzolato, G.; Ren, Y.; Thakkar, K.; Wovkulich, P.; Zhang, Z. 7,8-Disubstituted pyrazolobenzodiazepines. U.S. Patent 7,524,840, 2009.
- (23) Fabian, M. A.; Biggs, W. H.; Treiber, D. K.; Atteridge, C. E.; Azimioara, M. D.; Benedetti, M. G.; Carter, T. A.; Ciceri, P.; Edeen, P. T.; Floyd, M.; Ford, J. M.; Galvin, M.; Gerlach, J. L.; Grotzfeld, R. M.; Herrgard, S.; Insko, D. E.; Insko, M. A.; Lai, A. G.; Lelias, J.-M.; Mehta, S. A.; Milanov, Z. V.; Velasco, A. M.; Wodicka, L. M.; Patel, H. K.;

- Zarrinkar, P. P.; Lockhart, D. J. A small molecule-kinase interaction map for clinical kinase inhibitors. *Nat. Biotechnol.* **2005**, 23, 329–336.
- (24) Goldstein, D. M.; Nathanael, S.; Gray, N. S.; Zarrinkar, P. P. High-throughput kinase profiling as a platform for drug discovery. *Nature Rev. Drug Discovery* **2008**, *7*, 391–397.
- (25) Tovar, C.; Higgins, B.; Deo, D.; Kolinsky, K.; Liu, J. J.; Heimbrook, D. C.; Vassilev, L. T. Small-molecule inducer of cancer cell polyploidy promotes apoptosis or senescence: Implications for therapy. *Cell Cycle* **2010**, *9*, 3364–3375.
- (26) Kolinsky, K.; Tovar, C.; Zhang, Y.-E.; Railkar, A.; Yang, H.; Carvajal, D.; Nevins, T.; Geng, W.; Linn, M.; Packman, K.; Liu, J. J.; Zhang, Z.; Wovkulich, P.; Ju, G.; Higgins, B. Preclinical evaluation of the novel multi-targeted agent R1530. *Cancer Chemother. Pharmacol.* 2011, 68, 1585–1594.